



## Results of an international benchmark study on numerical simulation of flooding and motions of a damaged ropax ship

Pekka Ruponen<sup>a,b,\*</sup>, Petri Valanto<sup>c</sup>, Maria Acanfora<sup>d</sup>, Hendrik Dankowski<sup>e</sup>,  
Gyeong Joong Lee<sup>f</sup>, Francesco Mauro<sup>g</sup>, Alistair Murphy<sup>g,h</sup>, Gennaro Rosano<sup>d</sup>, Riaan van't Veer<sup>i</sup>

<sup>a</sup> NAPA, Finland

<sup>b</sup> Department of Mechanical Engineering, Marine Technology, Aalto University, Finland

<sup>c</sup> HSVA, Germany

<sup>d</sup> University of Naples Federico II, Italy

<sup>e</sup> University of Applied Science Kiel, Germany

<sup>f</sup> KRISO, Republic of Korea

<sup>g</sup> Maritime Safety Research Centre, University of Strathclyde, UK

<sup>h</sup> Brookes Bell, UK

<sup>i</sup> MARIN, The Netherlands

### ARTICLE INFO

#### Keywords:

Damage stability  
Validation  
Transient flooding  
Capsize  
Model tests  
Water on deck

### ABSTRACT

Survivability of damaged ships, especially ro-ro/passenger (ropax) vessels, is of paramount interest. Nowadays, time-domain simulation of flooding and motions of damaged ships are more frequently performed to obtain a more realistic overview of the actual survivability in case of a flooding accident. An international benchmark study on simulation of flooding and motions of damaged ropax vessels was conducted within the EU Horizon 2020 project FLARE, using new dedicated model tests as a reference. The test cases include transient flooding in both calm water and in irregular beam seas, as well as gradual flooding and capsizing in beam seas. The studied damage case is a two-compartment collision damage, and the studied intact metacentric height values were lower than the statutory requirements to achieve also capsizing cases. Numerical results were carefully compared against measurement data from the model tests. In transient flooding cases the capsize conditions were generally detected well by most codes. However, much variation was observed in the internal flooding and capsize mechanisms. For gradual flooding in beam seas, the results for capsize rate and time-to-capsize were characterized by significant variability among the codes. Results indicate that more research is needed to further improve the time-domain flooding simulation methods to correctly capture both transient flooding phenomena and motions of damaged ship in high waves.

### 1. Introduction

Ro-ro ships are known to be vulnerable if the large open vehicle deck is flooded, and already the early experimental research on damage stability in waves by Middleton and Numata (1970) studied capsizing of a damaged ship in waves with large, flooded compartments. Later (Bird and Browne, 1974) focused on a ro-ro/passenger (nowadays known as ropax) ship model. The tragic accidents of the *Herald of Free Enterprise* in 1987 and the *Estonia* in 1994 further motivated model tests on accumulation of water on deck, such as Pucill and Velschou (1990), Dand (1991), Damsgaard and Schindler (1996), Molyneux et al. (1997) and Chang and Blume (1998). Thereafter, the so-called Stockholm

Agreement model tests have been conducted especially for many existing ropax vessels, Schindler (2000), and also numerical simulation methods for the water on deck problem were developed, e.g. Chang (1999) and Vassalos (2000). During the past two decades, there has been extensive development in numerical tools for simulation of the flooding process and motions of damaged ships. An overview of these advancements was presented by Papanikolaou (2007), and subsequent progress is discussed in the review papers by Bačkalov et al. (2016) and Manderbacka et al. (2019).

Transient asymmetric flooding of damaged compartments was initially introduced in Spouge (1986) as an explanation for the rapid capsizing of the ferry *European Gateway* in 1982. The first model tests on

\* Corresponding author.

E-mail address: [pekka.ruponen@napa.fi](mailto:pekka.ruponen@napa.fi) (P. Ruponen).

<https://doi.org/10.1016/j.apor.2022.103153>

Received 12 October 2021; Received in revised form 22 March 2022; Accepted 23 March 2022

Available online 30 March 2022

0141-1187/© 2022 The Author(s). Published by Elsevier Ltd. This is an open access article under the CC BY license (<http://creativecommons.org/licenses/by/4.0/>).

**Table 1**  
Main dimensions of the studied ropax vessel.

	Full scale	Model scale
Length over all	About 162 m	About 5.8 m
Length between perpendiculars	146.72 m	5.24 m
Breadth	28.0 m	1.00 m
Draught	6.1 m	0.218 m
Height of ro-ro deck from baseline	9.2 m	0.329 m
Height of tank top from baseline	1.5 m	0.054 m
Gross tonnage	28 500	-

transient flooding were conducted with a simplified geometry, Vredeltd and Journée (1991), and later also for ropax vessels, e.g. by Journée et al. (1997) and de Kat et al. (2000). A comprehensive review of the characteristics and entailed factors of transient and progressive flooding stages of damaged ro-ro vessels is given in Khaddaj-Mallat et al. (2011), emphasizing flooding of the large open main vehicle deck and possible transient flooding effects. More recently, studies on transient flooding with simplified model geometries, by Lorkowski et al. (2014) and Manderbacka et al. (2015), have focused on the dynamics of the floodwater in the compartments during the transient stage. In addition, the effects of the breach opening position and the internal arrangement of the flooded compartments in the steady state after transient flooding have recently been studied with model tests, Acanfora and De Luca (2016, 2017).

The previous benchmark studies on flooding and motions of damaged ships have been organized by the International Towing Tank Conference (ITTC), and reported by Papanikolaou and Spanos (2001, 2005) and van Walree and Papanikolaou (2007). The first two included also motions of damaged ropax vessels, while the third one focused on progressive flooding in a box-shaped model, Ruponen et al. (2007). An additional benchmark study with transient flooding of a ropax vessel was conducted within the EU FP6 project SAFEDOR, as reported by Papanikolaou and Spanos (2008). The analysis focused on the critical significant wave height for surviving the studied two-compartment damage case. In addition, several validation studies on individual codes with dedicated model tests, Lee et al. (2007), Hashimoto et al. (2017), Ypma and Turner (2019), or even full-scale flooding tests, Ruponen et al. (2010), have been published.

Considering the increased importance of time-domain flooding

simulations and the newly developed codes since the previous studies, a new and extensive benchmark study was conducted within the EU Horizon 2020 project FLARE. The first part focused on fundamental flooding mechanisms with captive models, Ruponen et al. (2021), concluding that most participants were able to properly simulate simple up- and down-flooding cases. In the case of extensive progressive flooding on a deck with complex arrangement, there was quite large variation in the simulation results, but the relevant phenomena were properly captured. It was also noted that CFD codes can produce realistic results on the details of the flooding progression. However, only codes based on either Bernoulli's equation or shallow water equations were sufficiently fast for use in practical assessment of flooding and survivability of damaged ships.

The benchmark study continues with flooding of a ropax vessel both in calm water and in irregular waves, using measurements from new dedicated model tests at HSVA. The main purpose is to study the capability of currently available simulation tools to assess survivability of damaged ropax vessels, considering both transient and gradual flooding.

## 2. Benchmark study

### 2.1. Ropax ship model

An unbuilt ropax design (about 28 500 GT) provided by Meyer Turku was used. Tests were carried out at HSVA with a model in scale 1:28. Main parameters of the ship are listed in Table 1 both in full scale and in model scale. The lines drawing of the bare hull is shown in Fig. 1. All dimensions and results are presented in full scale.

At the studied draft of 6.1 m the minimum GM value according to the current SOLAS Ch. II-1 requirements is 3.2 m. This ensures a good survivability level, and therefore, much smaller GM values have been used in the model tests to achieve also capsizes cases for proper benchmarking and validation of the numerical simulation codes.

The arrangement of the floodable compartments is shown in Fig. 2. There are no internal connections between the compartments. A two-compartment collision damage is studied, as described in detail in section 4. There is a casing on the port side of the centerline on the vehicle deck, having an impact on the accumulation of water on the deck in waves. All damaged compartments were ventilated through ventilation pipes in the compartment corners. Consequently, full ventilation is

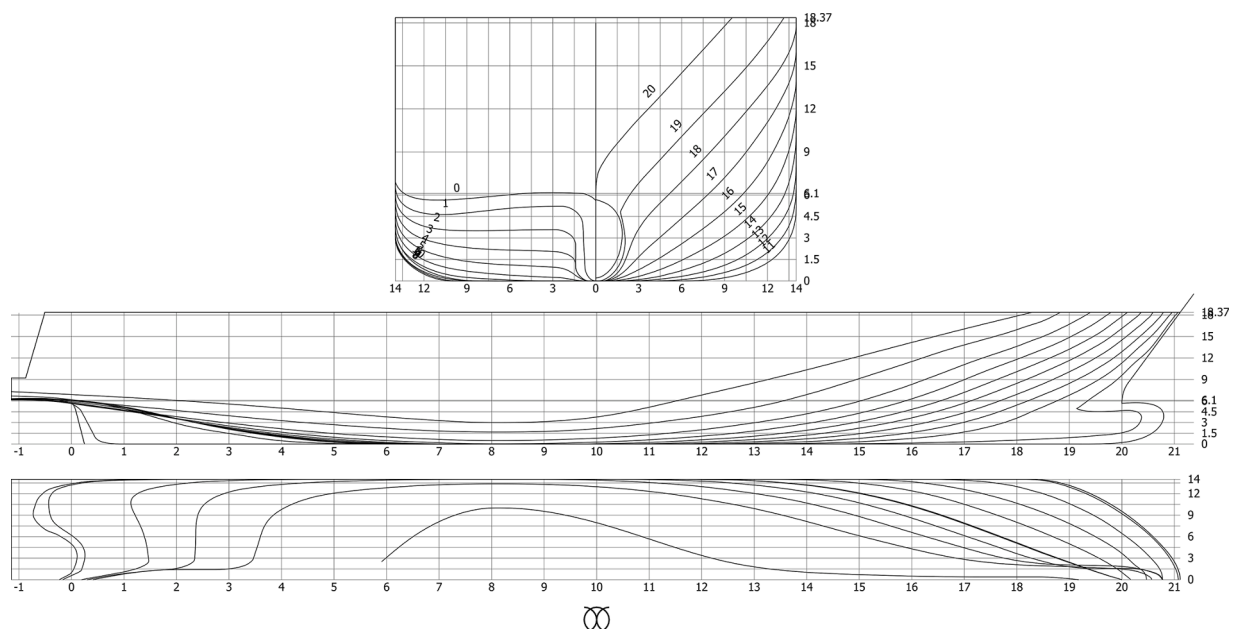


**Fig. 1.** Bare hull lines drawing of the studied ropax.

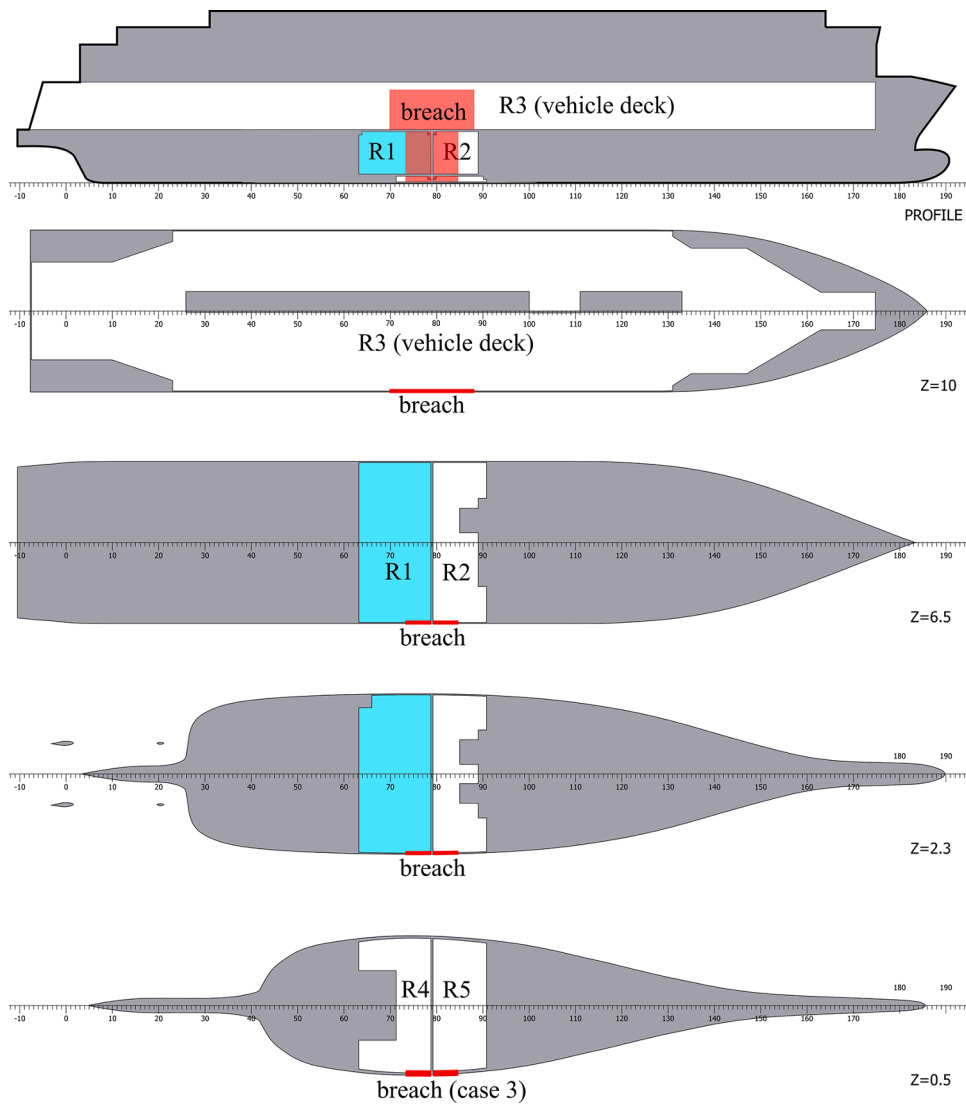


Fig. 2. Breach and floodable compartments of the ropax model; R1 is called “blue compartment”, frame spacing is 0.8 m.

Table 2

Summary of the participation in the benchmark study: the symbol ✓ indicates participation in the case.

ID	Participant	Code	Treatment of floodwater surface	Case 1: transient flooding in calm water	Case 2: transient flooding in waves	Case 3: gradual flooding in waves
BROO	Brooks Bell (UK)	PROTEUS	horizontal plane	✓	✓	–
HSVA	Hamburgische Schiffbau-Versuchsanstalt GmbH (GER)	HSVA-Rolls	Shallow water eqs.	✓	✓	✓
KRISO	Korea Research Institute of Ships & Ocean Engineering (ROK)	SMTTP	inclined plane	✓	✓	✓
MARIN	Maritime Research Institute Netherlands (NED)	XMF	inclined plane	✓	✓	✓
MSRC	Maritime Safety Research Center (UK)	PROTEUS	horizontal plane	✓	✓	✓
NAPA	NAPA (FIN)	NAPA	horizontal plane	✓	✓	–
UAK	University of Applied Science Kiel (GER)	E4	horizontal plane	✓	–	–
UNINA	University of Naples Federico II (ITA)	FloodW	inclined plane	✓	✓	–

assumed in the simulations. Due to the large scale (1:28) of the model, the openings are quite large, and therefore, the industry standard discharge coefficient 0.6 was recommended for all openings. All participants were provided a detailed 3D model of the hull geometry and internal compartments. The thickness of the decks and bulkheads, as well as some support structures, were also taken into account.

### 2.2. Test cases

The flooding process of a damaged ropax ship can involve various phenomena, that are investigated separately in the benchmark study:

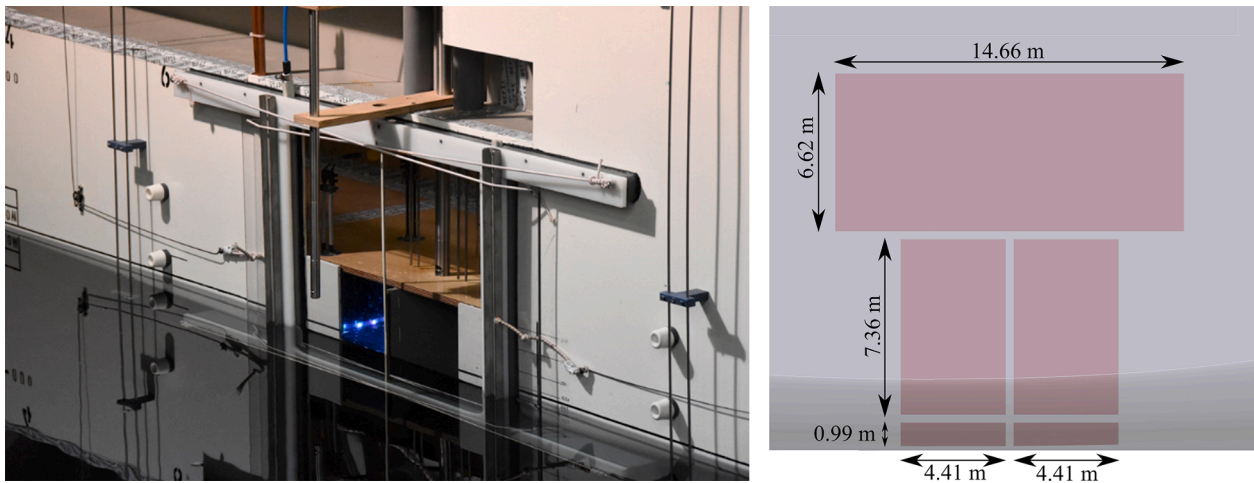


Fig. 3. Breach opening mechanism for the transient flooding tests (photo courtesy of HSVA) and full-scale dimensions of the breach.

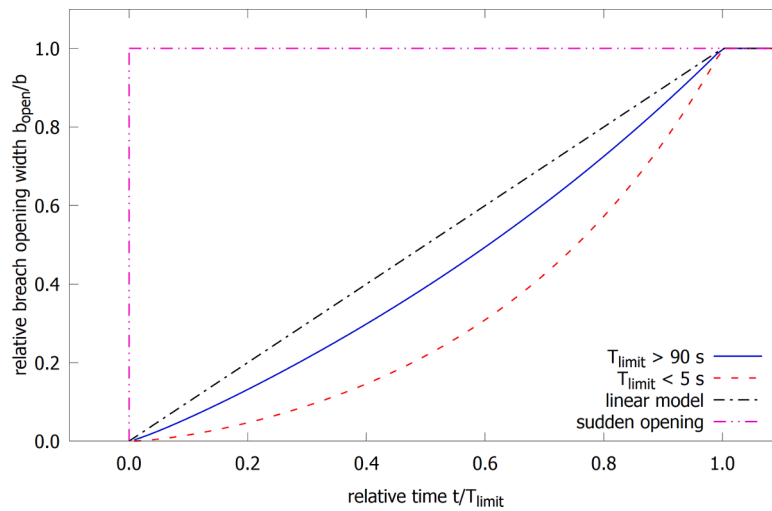


Fig. 4. Relative breach opening width as a function of time for the lower compartments.

Table 3

Natural roll period and logarithmic decrement parameters from the roll decay tests with an intact model for the initial conditions used in the benchmark study; values in full-scale; note that values in brackets were derived by interpolation.

GM (m)	Cases	Roll period (s)	$p$ (-)	$q$ (1/°)
1.338	1b, 1c	25.91	0.3658	0.02010
1.425	2a, 2b, 3a	(24.67)	(0.3612)	(0.02090)
1.505	1a	23.59	0.3565	0.02160
3.250	3b	15.84	0.1424	0.03545

1. Transient flooding in calm water with two different initial meta-centric height (GM) values (Cases 1a and 1b) and a third one (Case 1c) with slower opening time for the breach
2. Transient flooding in waves with two small variations in the initial steady heel angle (Cases 2a and 2b)
3. Gradual flooding of the vehicle deck in waves in two different sea states (Cases 3a and 3b)

All participants were provided with a detailed geometry of the ship and description of the benchmark cases. In addition, time histories of the measured roll motion for the transient flooding cases were shared in

Table 4

Comparison of hydrostatic and compartment data (full-scale).

Code ID	Buoyant hull up to T = 17.4 m				Volume of displacemet at T = 6.1 m				Floodable compartments				deck area m <sup>2</sup>
	V <sub>hull</sub> m <sup>3</sup>	X <sub>hull</sub> m	Y <sub>hull</sub> m	Z <sub>hull</sub> m	V <sub>disp</sub> m <sup>3</sup>	X <sub>disp</sub> m	Y <sub>disp</sub> m	Z <sub>disp</sub> m	V <sub>rooms</sub> m <sup>3</sup>	X <sub>rooms</sub> m	Y <sub>rooms</sub> m	Z <sub>rooms</sub> m	
BROO	61675	66.746	0.000	9.655	16186	67.851	0.000	3.456	29629	63.233	-0.135	12.012	3089.6
KRISO	61646	66.709	0.000	9.669	16084	67.963	0.000	3.458	29899	62.660	-0.131	12.031	3101.0
MARIN	61606	66.833	0.000	9.665	16118	68.019	0.000	3.457	29627	63.233	-0.135	12.013	3090.3
MSRC	61677	66.768	0.000	9.661	16163	67.817	0.000	3.458	29651	63.245	-0.129	12.003	3081.7
NAPA	61702	66.771	0.000	9.657	16189	67.838	0.000	3.455	29625	63.231	-0.135	12.013	3089.7
UAK	61667	66.790	0.000	9.660	16162	67.909	0.000	3.456	29871	63.445	-0.148	11.958	3093.6
UNINA	61683	66.790	0.000	9.660	16170	67.910	0.000	3.460	29627	63.233	-0.135	12.013	3090.3



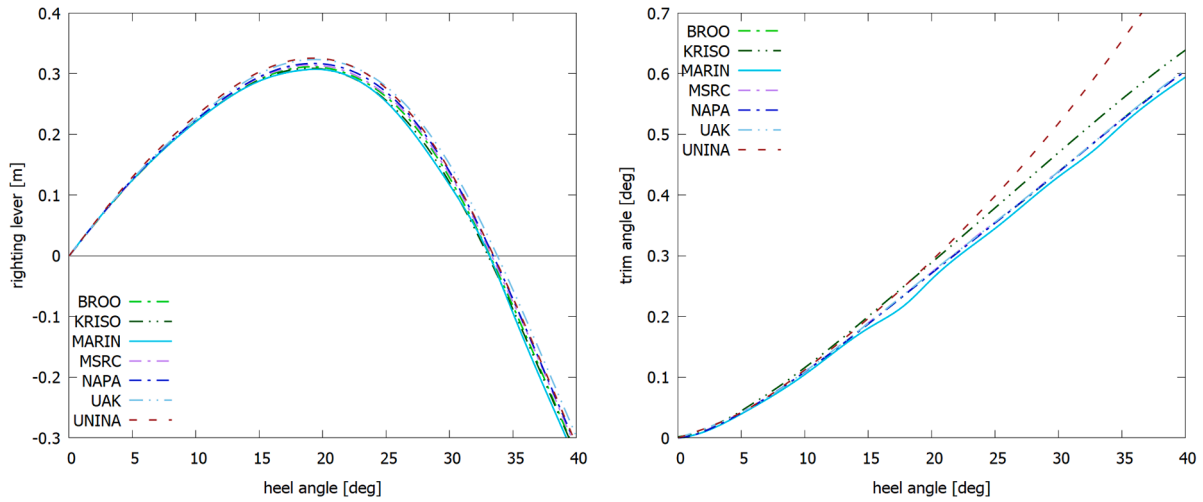


Fig. 5. Comparison of the righting lever curve (left) and trim angle (right) for an intact ship ( $GM = 1.505$  m) with different codes, bow trim is positive.

Table 5

Test cases and initial conditions for transient flooding in calm water (values in full-scale, bow trim and heel towards damage are positive).

Case	Description	GM (m)	Initial heel (°)	Initial trim (°)	Opening time $T_{limit, lower}$ breach (s)	Opening time $T_{limit, upper}$ breach (s)
1a	Stable final equilibrium	1.505	-0.78	0.30	2.96	3.81
1b	Capsize case	1.338	-0.52	0.30	1.80	2.54
1c	Slower opening time	1.338	-1.01	0.33	94.61	136.73

graphical format, to ensure fair and equal conditions for all participants.

### 2.3. Summary of participation

In addition to the FLARE partners, also other organizations with recent publications on flooding simulations were invited to the benchmark study. In total eight organizations participated, using seven different simulation codes. A summary of the participants is presented in Table 2, including the method used for treatment of floodwater. The

codes are mainly in-house software, developed at universities and research institutions. NAPA is a commercially available tool and PROTEUS, used by BROO and MSRC, is managed by Safety at Sea Ltd.

### 2.4. Applied simulation codes

All participants calculated the flow rates in the openings with a hydraulic model, based on Bernoulli’s equation. The methods for treatment of floodwater vary between the codes, as presented in Table 2. In general, these can be divided into three separate groups:

- Shallow Water Equations (SWE) with a discretized free surface,
- inclined plane, based on an apparent gravity (lumped mass) or a simplified dynamic resonance model,
- simplified model with the free surface modelled as a horizontal plane.

In addition, different approaches for considering the hydrodynamic forces were applied. A detailed description of each code, including applied methods, modelling, and references, is presented below.

BROO & MSRC

In-house code **PROTEUS** owned by Safety at Sea Ltd. Originally developed at University of Strathclyde (MSRC). Flooding rates are

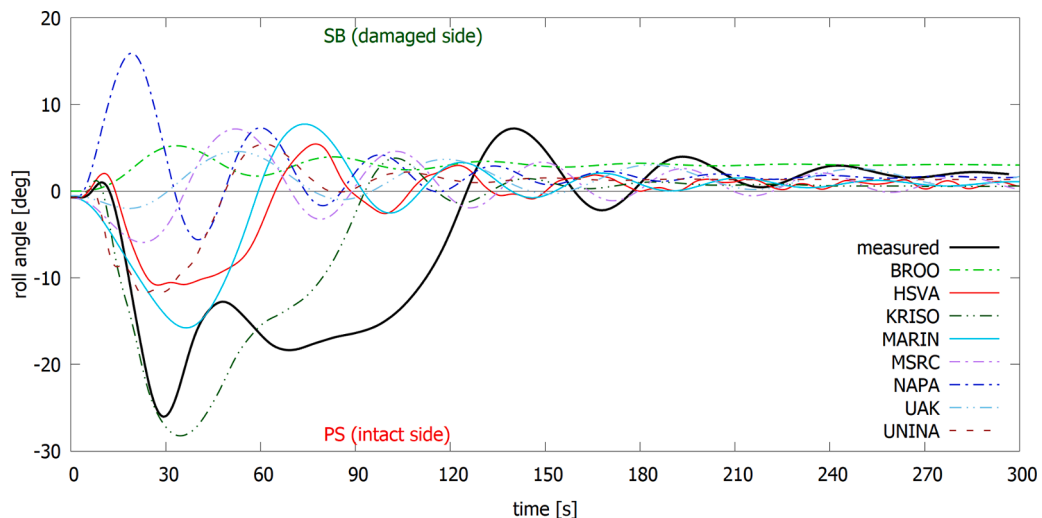


Fig. 6. Comparison of roll angle for transient flooding Case 1a with stable final equilibrium.

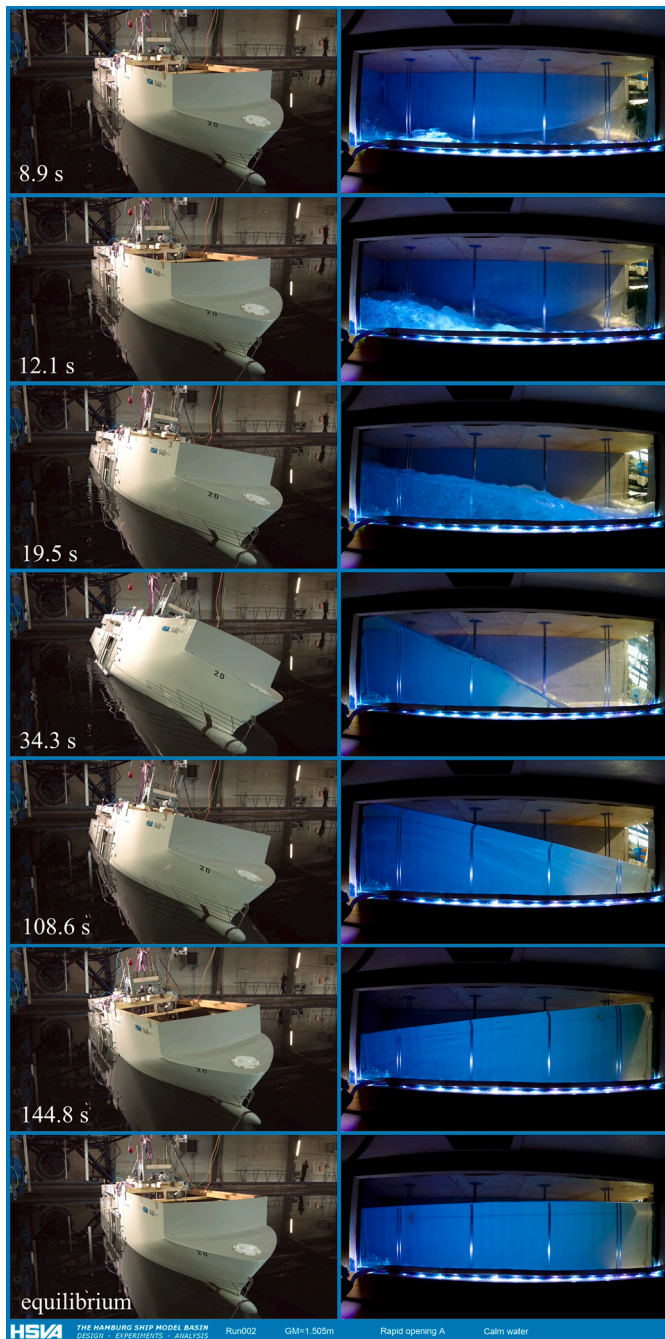


Fig. 7. Video captures showing the floating position and flooding of the “blue compartment” R1 in transient flooding in calm water, Case 1a, time stamps are in full scale; the compartment views show also the water level sensors.

calculated applying Bernoulli’s equation with a hard-coded discharge coefficient of 0.6. The code has a feature for Free-Mass-In-Potential-Surface (FMPS), Papanikolaou et al. (2000), where the whole mass of water in the compartment is treated as a single point mass. However, in this benchmark study, both MSRC and BROO used the current default setting, where the FMPS model is omitted, and the calculation assumes that the water level inside a compartment is always parallel to the undisturbed sea water level. Froude-Krylov and restoring forces are integrated up to the instantaneous wave elevation both for regular and irregular waves. Radiation and diffraction are derived from 2D strip theory. Hydrodynamic coefficients vary with the attitude of the ship during the flooding process (heave, heel and trim). Details are presented in Jasionowski (2001). In the test cases, motions were evaluated by

solving a 4 DOF system of equation (yaw and surge not modelled) assuming the vessel is allowed to drift freely. Hydrodynamic forces for the actual attitude of the vessel are obtained through interpolation on a precalculated set of forces obtained by 2D strip theory calculations. Drift forces are modelled according to empirical formulations. Compartments below the vehicle are considered as single rooms, while the vehicle deck has been divided at the centerline. Due to code limitations instant opening of the breaches was assumed in PROTEUS simulations, and consequently, BROO and MSRC did not provide results for the Case 1c.

#### HSVA

In-house version of the Rolls code, the **HSVA-Rolls** is used. Flood-water in internal compartments and decks can be modelled either with Shallow Water Equations (SWE) or with a pendulum model. For all cases in this study SWEs were used in all flooded spaces. Flow rates through the breaches are based on Bernoulli’s equation. For the ship heave, pitch, sway and yaw motions the method uses response amplitude operators (RAO) determined in the frequency domain with a linear strip method. The roll and surge motions are determined with time-integration using non-linear equations of motion coupled with the other four degrees of freedom (DOF), with hydrodynamic contributions based on linear strip theory and nonlinear hydrostatics in waves (based on NAPA calculations). Additional roll moments to this equation are provided by the flood water motions in the internal compartments. The vehicle deck R3 was discretized with a  $160 \times 30$  SWE grid resulting in altogether 3650 elements. In the transient Cases 1a to 1c rectangular  $24 \times 42$  and  $20 \times 56$  grids were used for the damaged R1 (‘blue’) and R2 compartments, respectively, whereas in the more gradual flooding Cases 2a to 3b in waves grid sizes of  $12 \times 28$  and  $10 \times 28$  for the R1 (‘blue’) and R2 compartments were used. In these cases the grid spacing was roughly 1.0 m for both longitudinal and transverse directions, whereas in the transient flooding cases finer grids in the two damaged compartments were found more appropriate.

#### KRISO

In-house code **SMTP** was used with flooding rates by Bernoulli equation and empirical discharge coefficients. The floodwater in compartments can be modeled either with a horizontal free surface or with a dynamic model in which the equation of motion of the mass center is solved using the tank resonance mode of the standing wave for the instantaneous water depth, and the resulting inclined free surface is used for the calculation of the pressure at openings. The compartments are treated independently, so the model can be selected appropriately to represent the property of each compartment. Ship motions are calculated by 6-DOF non-linear equations in time-domain, in which the Froude-Krylov and restoring forces are calculated for instantaneous wetted surface, and the hydrodynamic forces are calculated by the traditional strip method. The floodwater affects the ship motion as internal forces not as external forces, in other words, it changes the mass and its center of gravity resulting in changes of the inertial and gravity forces. Details are presented in Lee (2015a, 2015b). For this study, the large vehicle deck was divided into several compartments, and the dynamic resonance model of floodwater was selected for all compartments.

#### MARIN

The Extensible Modelling Framework (**XMF**) is a software toolkit on which all MARIN’s fast-time and real-time simulation software is based applying Newtonian dynamics, of which Fredyn and ANySim are known examples. XMF is recently extended with a flooding module library (XHL) based on Bernoulli’s equation with empirical discharge coefficients, using generic 3D defined floodable objects. A graph-solver technique is utilized to capture the complexity of entrapped air in compartments and for hydrostatic pressure-corrections from fully flooded compartments. To account for the flow inertia effects in the progression of flood water through the ship, the XMF framework is recently extended with a new inertia-based flow solver, denoted as the unified internal flow (UIF) module. The theory and first results of this solver are presented in van’t Veer et al (2021). The presented MARIN results were obtained by using the Bernoulli-based flow equations, while the free

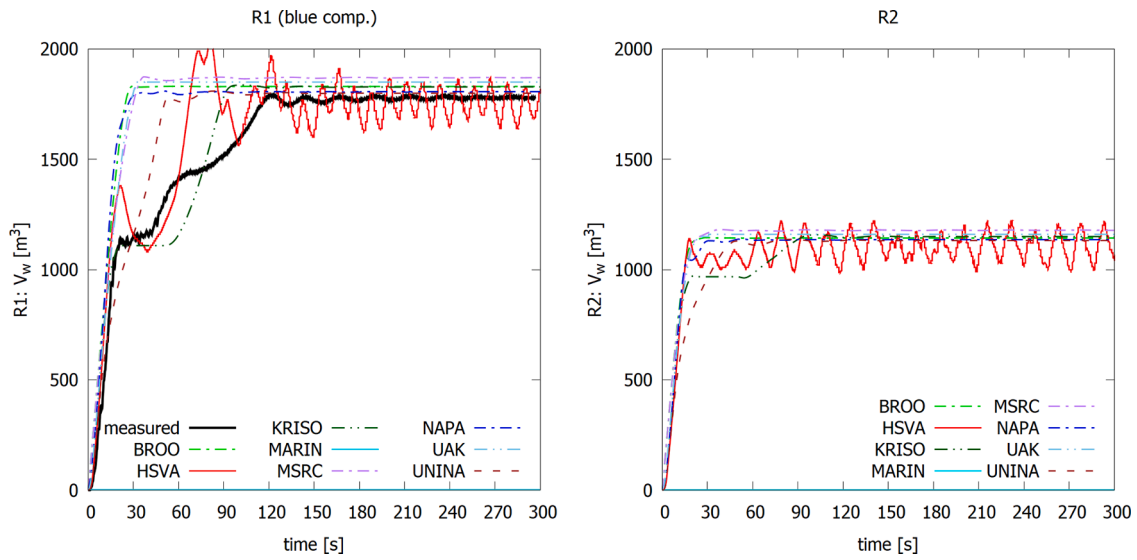


Fig. 8. Comparison of volumes of floodwater in transient flooding Case 1a with stable final equilibrium.

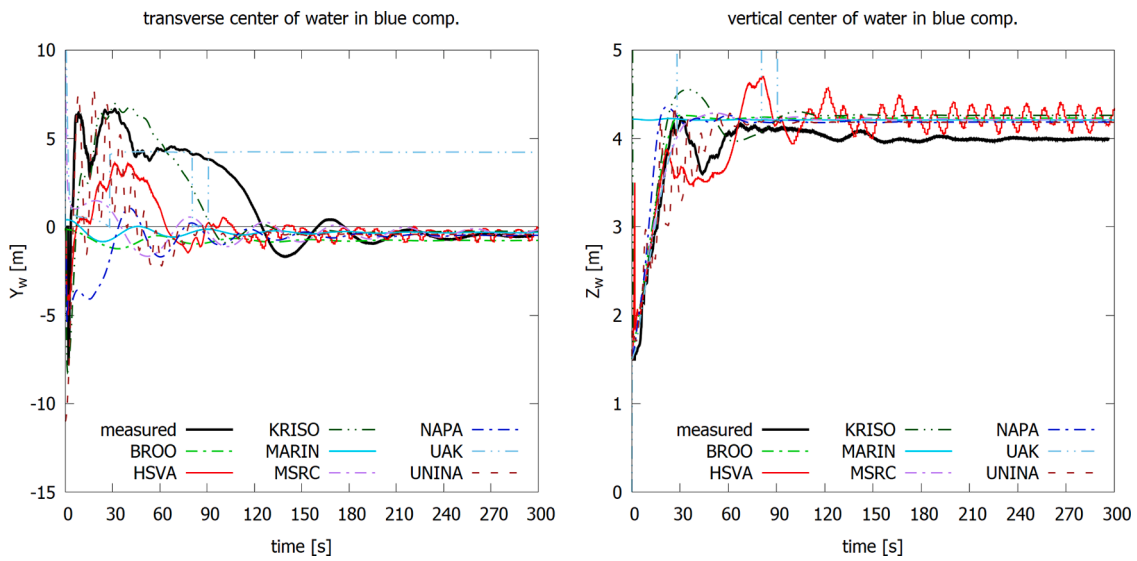


Fig. 9. Comparison of center of floodwater in the blue compartment R1 in transient flooding Case 1a with stable final equilibrium.

surface inclination due to the local effective gravity angle was used in the compartments R1 and R2. In other compartments a horizontal free surface was applied. The 6 DOF time domain solver is based on the convolution integrals, using memory functions obtained from frequency dependent hydrodynamic coefficients. The frequency domain hydrodynamic data was obtained from a linear 3D panel code PRECAL.

#### NAPA

The commercial software NAPA is used. The flow rates are calculated from Bernoulli's equation, with user-defined discharge coefficients for each opening. Horizontal free surface is assumed in all flooded rooms. Pressure-correction algorithm is applied to solve the governing equations (continuity and Bernoulli). Dynamic roll motion is solved with empirical user defined coefficients for intact ship. Draft and trim are treated as quasi-static. Effect of waves are considered only for flooding through the breach openings. Details are presented in Ruponen (2007, 2014). The simulation method is primarily intended for progressive flooding analyses. Since horizontal water levels are assumed, the two damaged compartments below the vehicle deck were divided at the centerline (CL), and the parts connected by a large opening (size equal to the intersection of the room at CL).

#### UAK

In-house code **E4 Flooding Method**, with flooding calculated by using Bernoulli's equation with horizontal surface and flooding path modelled as directed graphs. Ship motions either 3-DOF quasi-static or 6-DOF dynamic, with support for regular waves and other effects, e.g. interaction with cargo and seabed, Dankowski and Dilger (2013), conditional openings and leakage, Dankowski et al. (2014) and cargo shift. Details of the simulation method are presented in Dankowski (2013) and Dankowski and Krüger (2015).

#### UNINA

In-house tool **FloodW**, coded in Matlab-Simulink. Flooding rates are calculated based on Bernoulli's equation with empirical discharge coefficients. Floodwater is treated as lumped mass in agreement with the pendulum model. The position of the lumped mass, given the amount of floodwater and the free surface inclinations, depends on the tank geometry. The free surface is treated as a non-horizontal plane because normal to the so-called apparent gravity vector, (accounting for the instantaneous accelerations of the floodwater). Therefore, the free surface can have different inclinations from the ship roll and pitch angles. The code is able to perform 6-DOF simulations of the ship behavior both

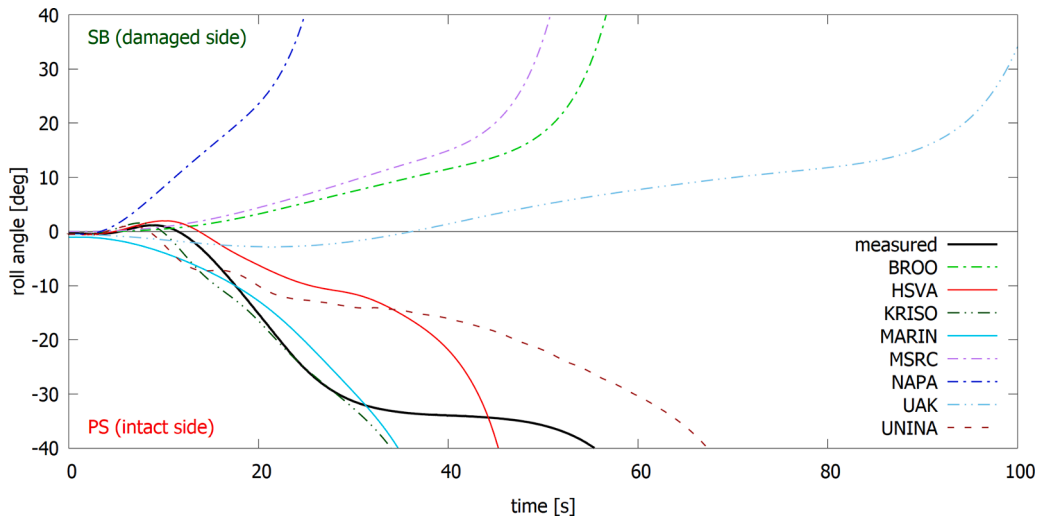


Fig. 10. Comparison of roll angle for transient flooding Case 1b with capsizes.

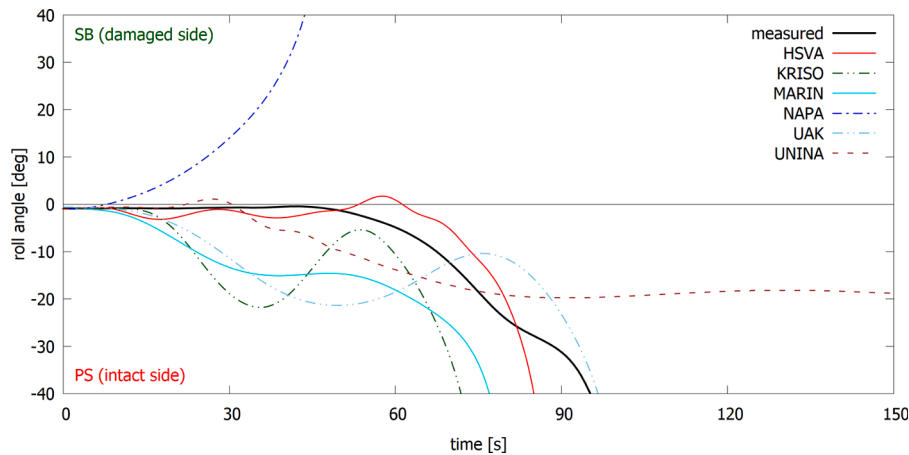


Fig. 11. Roll angle in transient flooding in calm water with slow opening of the breach, Case 1c.

Table 6

Initial conditions for transient flooding in waves (values in full-scale, bow trim and heel towards damage are positive).

Case	Initial heel (°)	Initial trim (°)	Opening time $T_{limit}$ , lower breach (s)	Opening time $T_{limit}$ , upper breach (s)
2a	1.15	0.47	2.08	2.86
2b	-0.39	0.45	2.22	2.96

in intact and damaged conditions. The hull is discretized into panels. Regular and irregular wave effects are modelled, accounting for all relevant nonlinearities, Acanfora and Rizzuto (2019). Details are presented in Acanfora and Cirillo (2016, 2017) and Acanfora et al. (2019).

### 3. Model tests

#### 3.1. Damage case

The examined damage is a collision breach on the starboard side, extending to two watertight compartments. The breach opening consists of two rectangles, one below the main vehicle deck and one above. Only the side shell is removed from the model, as shown in Fig. 3, and there are no cuts in the decks or bulkheads. In the transient flooding tests (Cases 1 and 2) the breach is initially closed by two sliding doors, and the double bottom rooms (R4 and R5) are intact. In the tests for gradual

flooding in waves (Case 3) the whole breach is open and all the compartments below the vehicle deck (R1, R2, R4 and R5) are already flooded, i.e. open to sea, when the test begins.

In the transient flooding tests (Cases 1 and 2), the breach is initially closed by two sliding doors. When the test begins, both doors slide away from the transverse bulkhead (see Fig. 3), and the widths of the breaches to the compartments increase. The breach opening mechanism in the model tests was operated with elastic bands. The sliding doors had some inertia and also the static friction in the system was bound to be higher than the sliding friction. For these reasons, the rate of opening was not completely linear and depends on the opening time  $T_{limit}$  of the lower compartments (R1 and R2). Based on detailed analyses at HSVA, the open width of the breach to these compartments in the case of rapid opening,  $T_{limit} < 5.0$  s is approximately:

$$b_{open}(t) = b \cdot \left( \frac{t}{T_{limit}} \right)^{1.7 + \frac{t}{T_{limit}}} \quad (1)$$

where  $b$  is the total width of the breach opening, as presented in Fig. 3. For slow opening process,  $T_{limit} > 90.0$  s:

$$b_{open}(t) = b \cdot \left( \frac{t}{T_{limit}} \right)^{1.2 + 0.3 \frac{t}{T_{limit}}} \quad (2)$$

The times are given in full scale. Both functions, along with a linear assumption, are presented in Fig. 4. Due to code limitation, BROO and



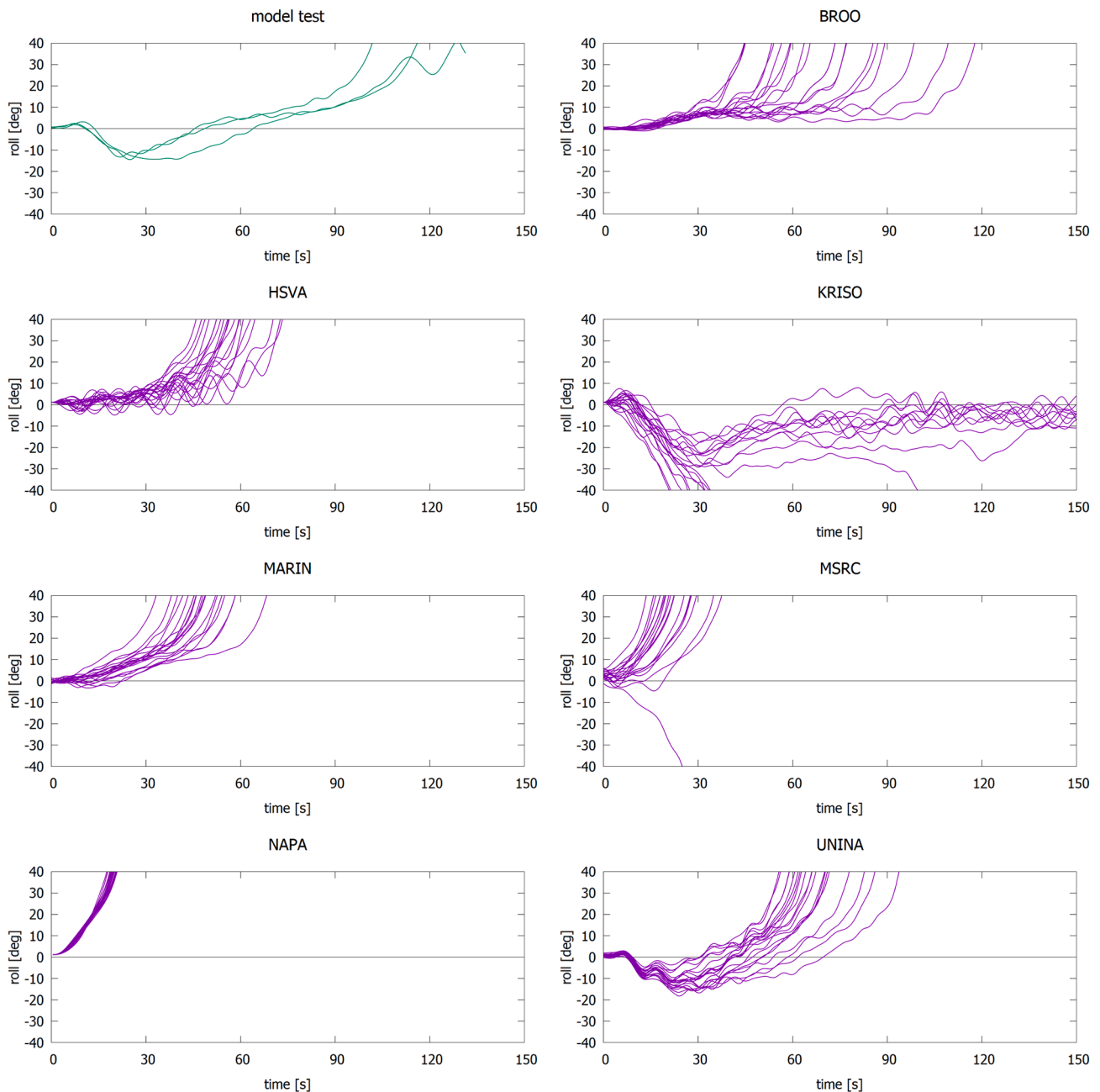


Fig. 12. Development of roll angle in transient flooding with small initial heel towards the damage (Case 2a).

MSRC modelled breaches to be suddenly opened. KRISO, MARIN, NAPA and UAK applied the linear model, whereas HSVA and UNINA used the approximate functions, (1) and (2). The opening time of the breach to the vehicle deck is less important in the studied transient flooding cases since in the benchmark cases it is not submerged until the doors are fully open. For each transient flooding case, the  $T_{limit}$  values are given in tables in the following sections.

### 3.2. Test setup and measurements

All the tests were conducted for a freely drifting model. For the tests in waves, bow and stern lines were occasionally used to correct the model orientation back to beam seas condition. For practical reasons, the roll angle of  $36^\circ$  was used as the nominal limit for capsizing, and the test was interrupted when the roll angle exceeded this limit.

The model was equipped with instruments to measure the 6 Degrees-of-Freedom motions, the relative wave elevations at several positions on and below the main vehicle deck. All data were recorded at a sampling rate of 100 Hz in model scale, which corresponds to 18.9 Hz in full scale.

Four video cameras were used to record the tests, two outside cameras focusing on the ship motions, one recording the water elevation in the compartment R1 below the main vehicle deck, and one showing water ingress to the vehicle deck (room R3).

For transient flooding cases the volume of water and its centroid in the blue compartment R1 were analyzed by HSVA based on the six water level sensors in the compartment. These sensors were located transversally, and therefore, the analysis is based on the assumption of two-dimensional water surface.



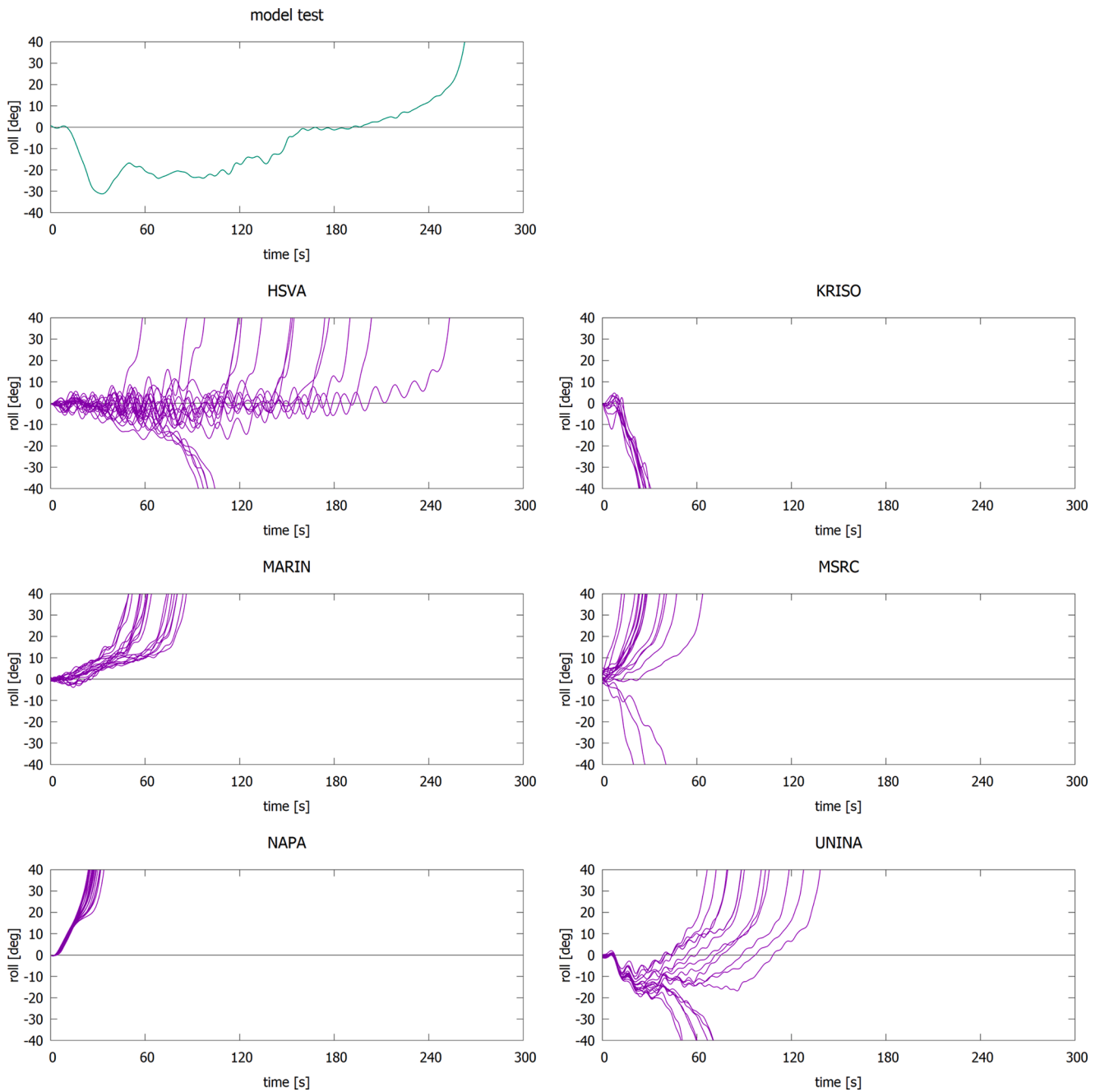


Fig. 13. Development of roll angle in transient flooding with small initial heel away from the damage (Case 2b).

### 3.3. Roll damping characteristics

The model included shaft lines, rudders, and bilge keels. In the tests with transient flooding (Cases 1 and 2), the bilge keels on the starboard side were removed to compensate the additional roll damping of the door supporting frame (see Fig. 3). Roll decay tests were conducted by HSVA for an intact model with the bilge keels and other appendages, and the results presented in Table 3, were provided beforehand to all participants. For roll damping characteristics, the logarithmic decrement:

$$\Lambda = \ln(\phi_{a,i} / \phi_{a,i+1}) \quad (3)$$

where  $\phi_{a,i}$  and  $\phi_{a,i+1}$  are roll amplitudes (separated by one roll period), was provided as a linear fit:

$$\Lambda(\phi_a) = p + q\phi_a \quad (4)$$

The coefficients  $p$  and  $q$  are given in Table 3, along with the measured roll period. For  $GM = 1.425$  m (in Cases 2a, 2b and 3a) interpolated values were used, as indicated in Table 3.

### 4. Comparison of hydrostatics

In order to ensure that all participants had modelled the hull form and floodable compartments accurately, some basic hydrostatic results were collected and checked beforehand, Table 4. Buoyant hull was considered to extend up to 17.4 m above the baseline. The volumes of the hull and displacement ( $V_{hull}$  and  $V_{disp}$ ), as well as the center of the buoyant hull ( $X_{hull}$ ,  $Y_{hull}$ ,  $Z_{hull}$ ) and the center of displacement at intact draft ( $X_{disp}$ ,  $Y_{disp}$ ,  $Z_{disp}$ ) were compared. In addition, the total volume and center of the floodable compartments ( $V_{rooms}$ ,  $X_{rooms}$ ,  $Y_{rooms}$  and  $Z_{rooms}$ ) were checked, as well as the deck area of the vehicle deck (room

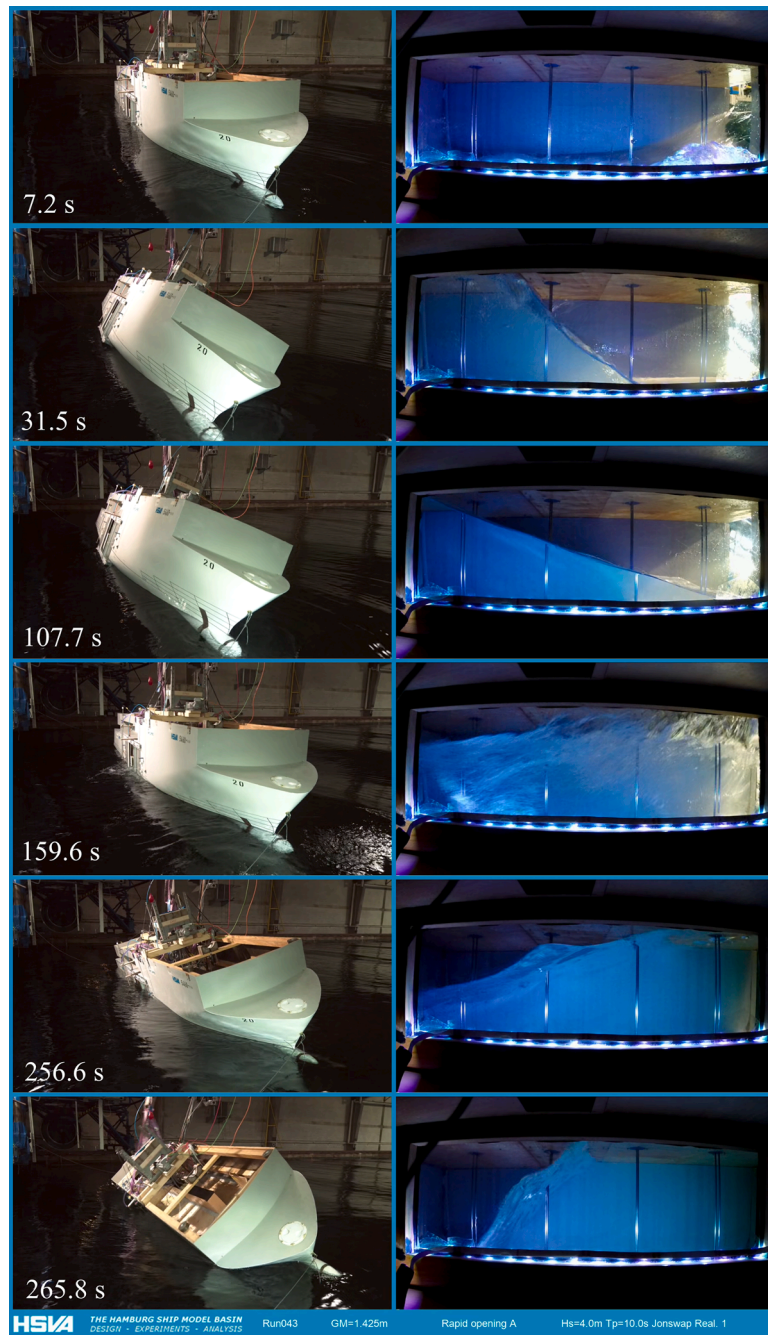


**Fig. 14.** Video captures showing the floating position and flooding of the “blue compartment” R1 in transient flooding in beam seas, with small initial heel away from the damage Case 2b, time stamps in full scale.

R3). No significant deviations in either volumes or the centroids between the different codes were found. Consequently, the numerical models of the ship are considered similar enough, and thus suitable for benchmarking.

Intact stability characteristics of the ship were compared at an upright condition with initial metacentric height of 1.505 m (in full scale). The righting lever curves and related trim angles, as calculated with different codes, are presented in Fig. 5. Some small variation at large heel angles can be observed, especially regarding the trimming of the ship. On the other hand, some curves are practically overlapping, and thus not clearly visible in Fig. 5. In general, the restoring moments are very similar. Moreover, the hull form is rather conventional, and there are no significant discontinuities in the waterplane area around the studied draft. Therefore, small differences in the modelling of the hull

form are not expected to have a notable effect on the hydrostatic quantities. It should be noted that the hydrostatics from HSWA were based on pre-calculated hydrostatics using NAPA Software, and hence they are not included in the comparison.

### 5. Transient flooding in calm water (Case 1)

With a low metacentric height, the transient flooding can cause a large roll even in calm water, and in a worst case this results in capsize. Moreover, the time frame when the breach is introduced can have notable effects on the transient response, de Kat et al. (2000). Consequently, three separate test cases were included. The initial condition for each case is listed in Table 5, based on measured floating position of the model just before flooding was initiated. It should be noted that all

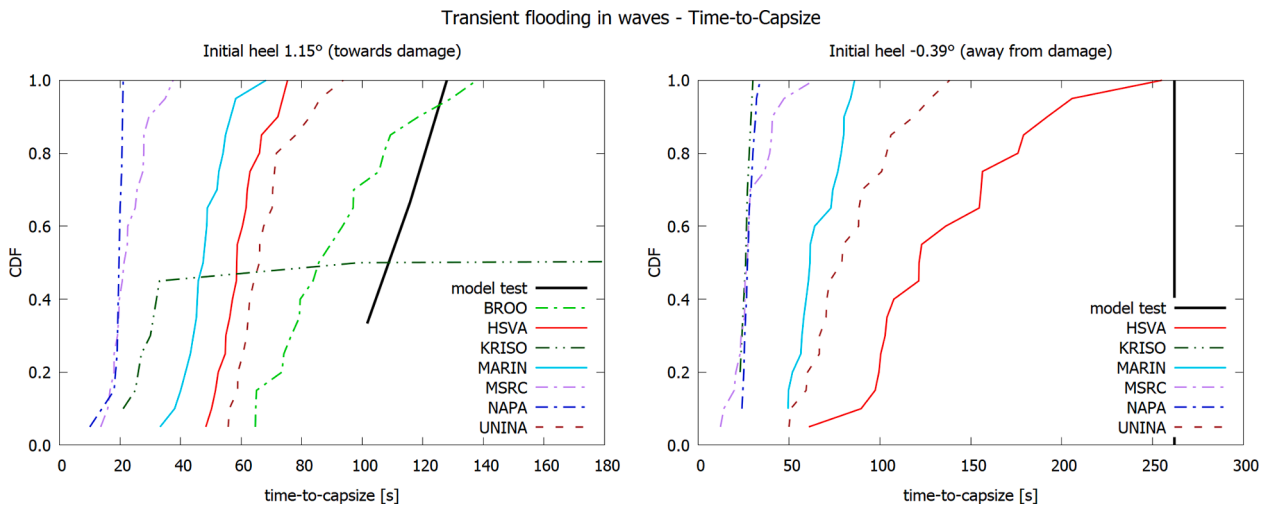


Fig. 15. Cumulative time-to-capsize for transient flooding in waves with different initial heel angles, Case 2a on left and Case 2b on right.

Table 7

Test cases for gradual flooding in waves.

Case	$H_s$ (m)	$T_p$ (s)	Intact draft (m)	Intact GM (m)
3a	3.5	10.0	6.10	1.425
3b	7.5	10.0	6.10	3.250

studied GM values are significantly below the minimum value to pass the SOLAS Ch. II-1 requirements, in order to produce interesting phenomena, including a capsizing, for benchmarking purposes. It is also emphasized that the objective was not to investigate the real survivability of the ship design. Furthermore, Table 5 contains the times for opening the doors that cover the breach openings. The effective width of the breach as a function of time can be estimated by using equations (1) and (2). These can also be used for the upper part of the breach to the vehicle deck (room R3), but it is irrelevant since the whole breach was already open when this part of the breach was immersed in all test cases.

5.1. Transient flooding with stable final equilibrium (Case 1a)

In the first test case the ship has a low initial metacentric height  $GM = 1.505$  m (full scale), but it is still sufficient for achieving a stable equilibrium floating position after flooding. Before the test, the model had a small steady initial heel angle  $-0.78^\circ$  (away from the damage), and a zero initial roll velocity was applied as initial condition.

Initially the ship rolls towards the damage (positive roll angle) but the actual transient roll is towards the intact side (negative roll angle). After about 120 s (full-scale) the ship has recovered from the transient roll towards the intact side and starts to roll towards the damaged side. Eventually, the roll decays to a small stable heel angle towards the damage, see Fig. 6. Similar transient roll towards the intact side has been previously observed with a box-shaped barge model, Manderbacka et al. (2015).

The large transient roll towards the intact side is explained by the momentum of the in-flooding water, and possibly also with small initial

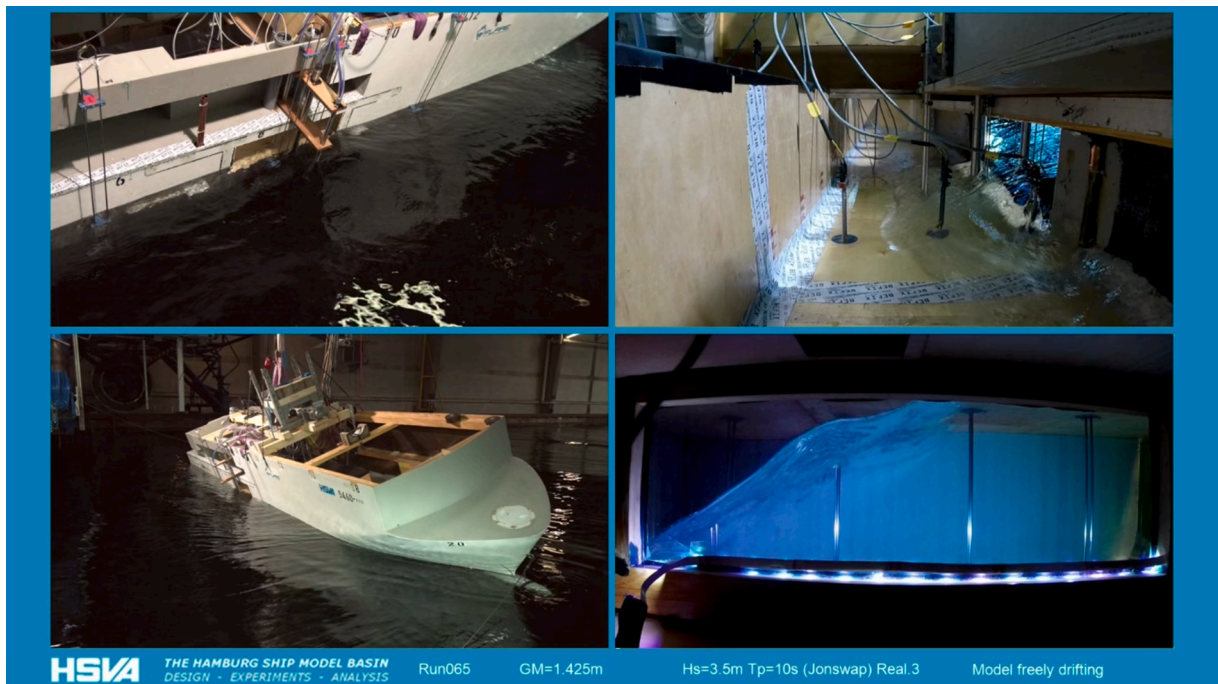


Fig. 16. Video capture on gradual flooding in beam seas (Case 3a) with  $H_s = 3.5$  m when the main vehicle deck is being flooded, resulting in capsizing.



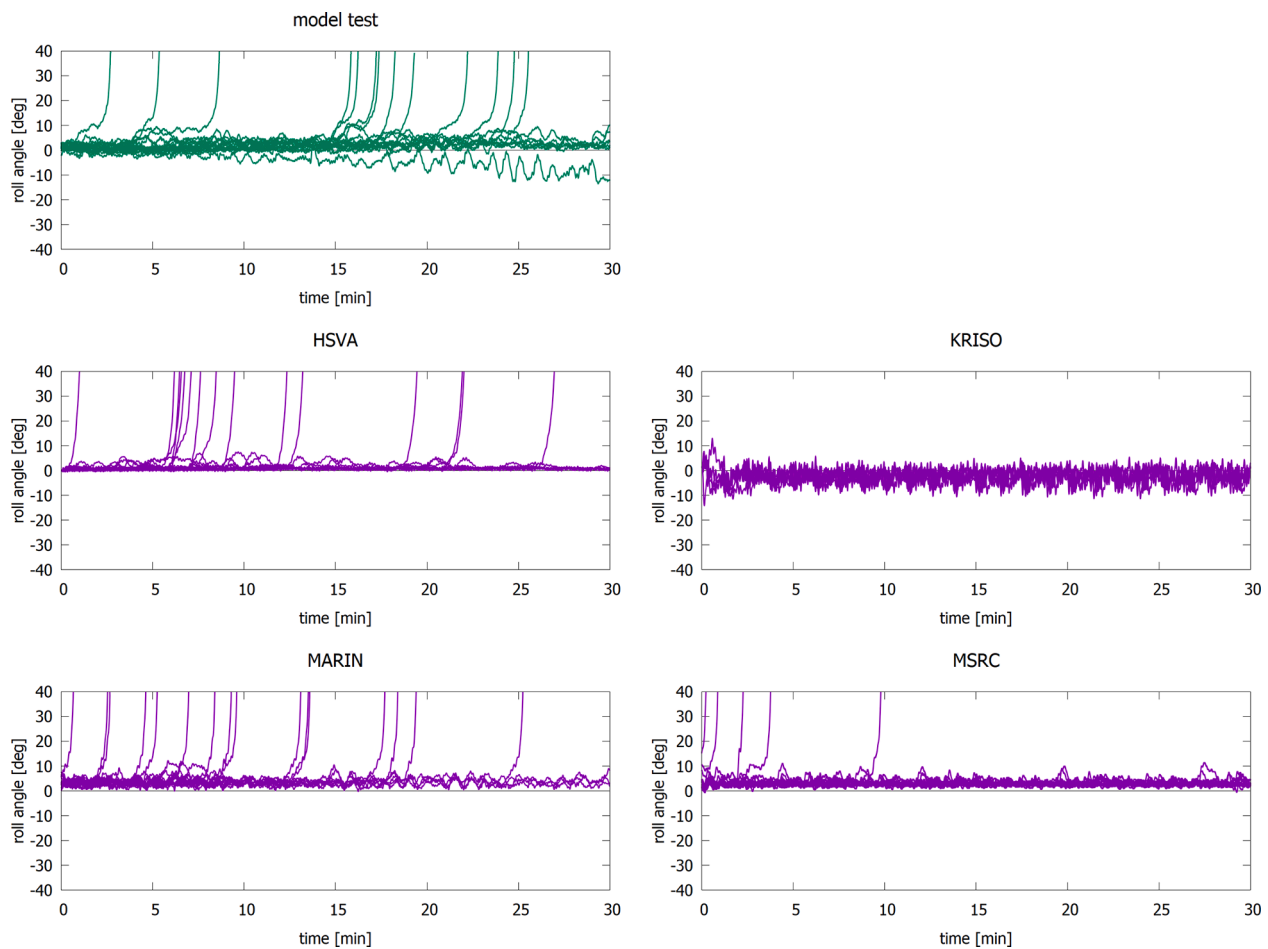


Fig. 17. Measured and simulated roll angle for 20 wave realizations for Case 3a with  $H_s = 3.5$  m.

heeling towards that side. Some video captures showing the floodwater in the “blue compartment” R1 and the corresponding floating position of the model are presented in Fig. 7. It can be clearly seen that floodwater initially accumulates on the intact side of the compartment. HSVA has analyzed the time histories for the volume and center of floodwater in R1, based on the signals from six water level sensors in this compartment. Comparisons of the volumes of floodwater in both compartments R1 and R2 are shown in Fig. 8 and for the center of floodwater in R1 in Fig. 9.

The code by KRISO predicts the trend of the development of roll motion very well, only the peak angle is slightly overestimated. Also HSVA, MARIN and UNINA capture the transient heeling towards the intact side, but the magnitude is notably smaller. HSVA, KRISO and UNINA also capture the small initial roll towards the damage before the larger transient roll towards intact side, whereas MARIN predicts roll towards intact side from the beginning of the flooding. MSRC predicts the initial roll direction to intact side correctly, but the peak is about 20° smaller than measured. BROO used the same code but applied zero initial heel, resulting in transient roll towards the damage. Also UAK predicts similar development of roll, but with smaller magnitude than MSRC. Similarly, the quasi-static flooding model in NAPA predicts a transient roll towards the damage.

There is some variation in the final equilibrium heel angle, however, in general, the results are rather consistent, especially when considering the low initial GM of the ship and extensive flooding.

The underestimation of the transient roll towards the intact side results in too fast flooding of the breached compartments, see Fig. 8. Comparison of the transverse center of floodwater in the compartment R1, Fig. 9, explains the observed results in the roll angle with different

codes. It is also noted that the HSVA simulation, based on SWE, results in larger oscillations in the volumes of floodwater than the simulations with other codes assuming either horizontal or inclined flat water surface in the compartments.

### 5.2. Capsize during transient flooding (Case 1b)

In the second transient flooding case, the initial metacentric height was lowered to  $GM = 1.338$  m, which is low enough to cause a capsize in calm water. Before the test, the model had a small stable initial heel angle  $-0.52^\circ$  (away from the damage) and trim angle of  $0.30^\circ$  (to bow). The lower part of the breach was opened in 1.80 s (full scale) and the breach of the vehicle deck in 2.54 s. The comparison of measured and simulated roll angles is shown in Fig. 10. Roll motion towards the damage is minimal, and after about 12 s (full scale) the ship starts to roll towards the intact side and capsizes in about 55 s.

HSVA, KRISO and UNINA can correctly capture small initial roll towards the damage and the subsequent roll away from the damage, although there is quite notable difference in the actual time-to-capsize. Also MARIN predicts well the capsize towards the intact side but the small initial roll towards the damage is not captured. BROO and MSRC simulations result in roughly correct time-to-capsize, but the ship capsizes towards the damaged side. Both participants used the same PROTEUS code, and their difference in the TTC is likely caused by the different initial condition since BROO applied zero initial heel and MSRC considered the small initial heel angle. Also NAPA predicts capsize towards the damaged side, with too short TTC. UAK estimates initial roll towards the intact side, but this is slowly equalized, and eventually the ship capsizes towards the damaged side with significantly

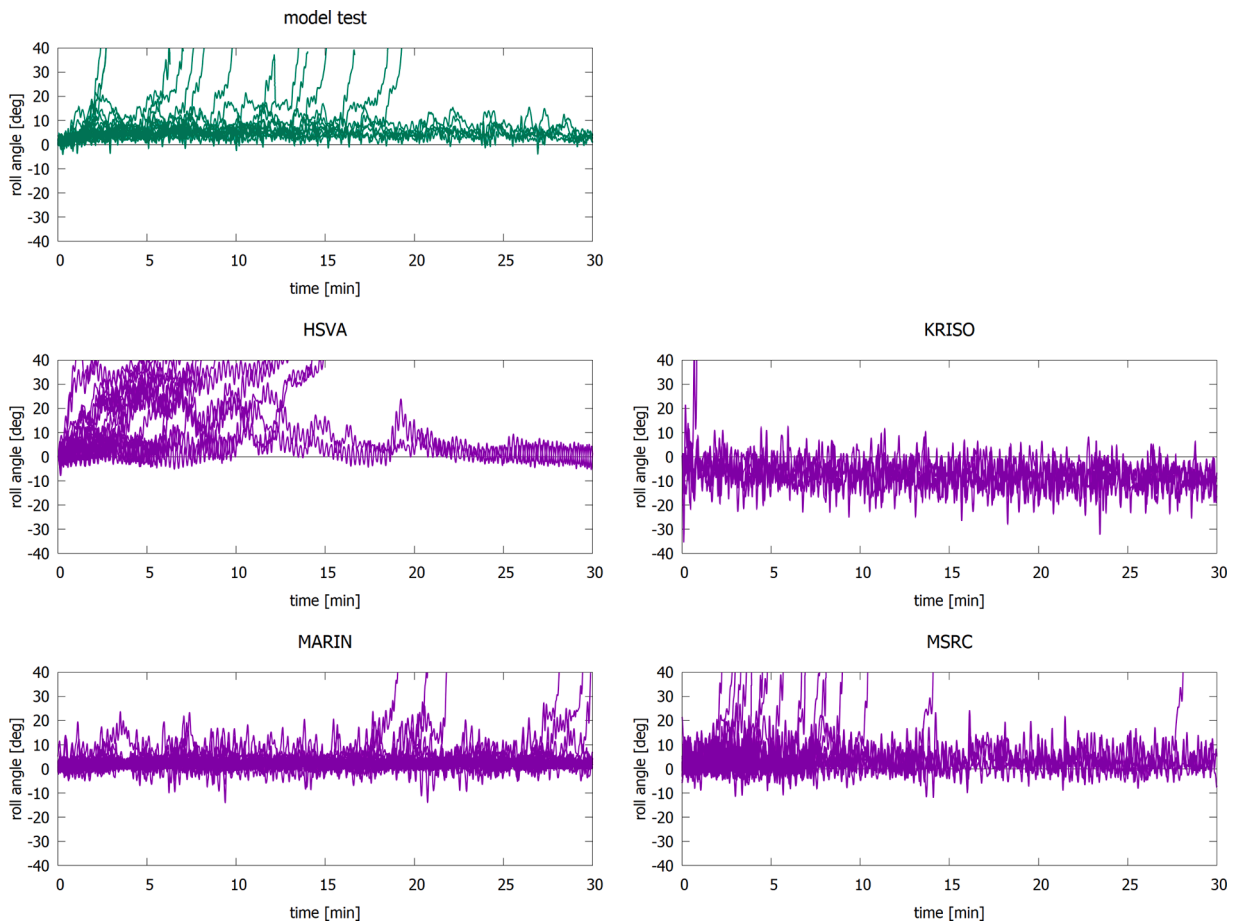


Fig. 18. Measured and simulated roll angle for 20 wave realizations for Case 3b with  $H_s = 7.5$  m.

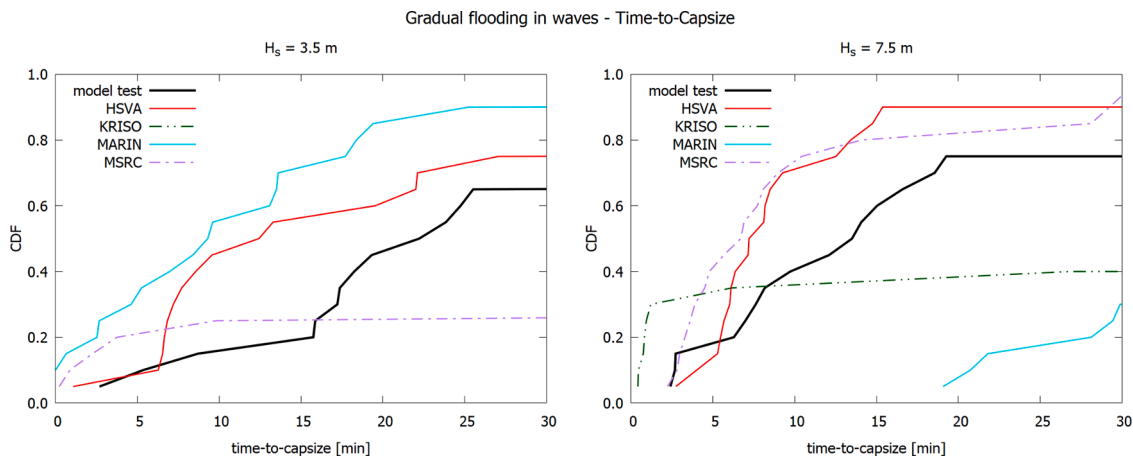


Fig. 19. Cumulative distribution of time-to-capsize (TTC) for Case 3a with  $H_s = 3.5$  m (left) and for Case 3b with  $H_s = 7.5$  m (right).

Table 8

Capsize rate from 20 repetitions in the same sea state for 30 min (full scale).

Case	$H_s$	Model tests	HSVA	KRISO	MARIN	MSRC
3a	3.5 m	65 %	75 %	0 %	90 %	25 %
3b	7.5 m	75 %	90 %	40 %	30 %	95 %

slower TTC than in model test.

### 5.3. Transient flooding with slow opening time for the breach (Case 1c)

Usually the studies on transient flooding, both experimental and numerical, rely on the assumption that the breach is opened rapidly. However, for collision damages this is not fully realistic since the striking ship affects the initial flooding process. Previously, de Kat et al. (2000) have observed from model tests that the opening time has a notable effect on the transient roll angle. Yet in most model tests on



transient flooding the breach is opened very rapidly, and the standard practice in flooding simulations is to assume that this happens instantly. Consequently, in the third transient flooding test case the breach was opened slowly.

In this test case the stable initial heel angle of the model before the test was  $-1.01^\circ$  (away from the damage) and trim angle was  $0.33^\circ$  (to bow). The lower part of the breach was opened in 94.61 s (full-scale) and the upper part in 136.73 s (full-scale). The same initial condition as in the transient capsize Case 1b, with low GM = 1.338 m, was used.

The results for the roll angle are shown in Fig. 11. In the experiment, the roll angle remained minimal for over 40 s (full-scale), whereas in all simulations roll started to increase much faster. The capsize mechanism is in principle the same as with fast opening time of the breach, but the process is now much slower.

HSVA, KRISO, MARIN and UAK correctly capture the capsize towards the intact side, with fairly good estimate on the time-to-capsize. Also UNINA correctly predicts the direction of the roll motion, but instead of a capsize, a steady heel of about  $-20^\circ$  is achieved. The quasi-static treatment of floodwater in NAPA results in capsize towards the damage. Only HSVA manages to predict that the roll angle remains rather small for a long period of time, whereas with the other codes roll starts to increase much faster than in the experiment.

## 6. Transient flooding in waves (Case 2)

The second part of the benchmark study focuses on transient flooding in irregular beam seas. Relatively low initial GM of 1.425 m is applied. JONSWAP wave spectrum ( $\gamma = 3.3$ ) with  $H_s = 4.0$  m and  $T_p = 10.0$  s is used, with waves facing the damage. Two variants of the initial condition are studied, as listed in Table 6, with small variation, especially in the initial heel angle. These conditions were determined by HSVA from the heave, roll and pitch signals, averaged over the time range of 10 s (model scale) in calm water before the wave met the model.

Several experiments were conducted for transient flooding in beam seas. In three cases the initial condition before flooding was practically the same (Case 2a). Analysis of experimental data showed large variation for cases with slightly different initial condition, and therefore an additional Case 2b was included in the benchmark study. Participants were asked to provide simulation results for 20 random wave realizations for both studied initial conditions. Eventually, BROO provided results only for zero initial heel angle and KRISO submitted only 10 realizations for the latter condition since the time-to-capsize was very consistent with a smaller number of repetitions. Each participant used their own codes for generating the waves.

Time histories for the roll motion with the two initial conditions are shown in Fig. 12 and Fig. 13. As in the case of transient flooding in calm water, Fig. 6 and Fig. 10, the ship initially rolls towards the damage, which is followed by large transient roll away from the damage. However, in contrary to the calm water case, this transient roll does not result in capsize, due to slightly larger intact GM. The whole breach opening is temporarily emerged from water, but waves cause further flooding, and the ship starts to slowly roll towards the damage, eventually capsizing to this direction. Video captures from the model tests of the Case 2b in Fig. 14 visualize this process.

KRISO predicts capsize towards the intact side, and in the Case 2a the ship survives the large transient flooding stage in several realizations of the studied sea state. With other codes, capsize towards the damage is more common, but also HSVA, MSRC and UNINA predict capsize towards the intact side in some wave realizations in the Case 2b. Cumulative distributions for time-to-capsize are presented in Fig. 15. BROO used zero heel as initial condition, whereas other participants applied the measured initial heel and trim. In the Case 2a, HSVA, MARIN and NAPA simulations always capsize towards the damaged side, but with TTC significantly shorter than in model tests. The difference to the model tests is almost equal to the time the vessel remains heeling towards the intact side in the model tests, which is not seen in these

simulations. Based on the single experiment for the Case 2b TTC seems to be longer, but it is still much shorter than in the model tests. In general, the increase of TTC when the ship is initially heeling away from the damage is qualitatively captured well. However, variation in TTC between the codes is significant. For the Case 2a results of BROO are close to the measured TTC distribution, but this is partly explained by the different initial heel angle. Although with only one experiment for the Case 2b, it can be concluded that the codes by HSVA and UNINA seem to provide a qualitatively good estimate of both TTC and the development of roll motion. Moreover, in most realizations of the sea state, UNINA captures well the maximum transient roll angle towards the intact side before the final capsize towards damage, albeit there are some more oscillations in the roll motion than in the measurements. Similar excessive oscillations are visible also in the HSVA and KRISO simulations.

This part of the benchmark study clearly demonstrates that in certain flooding scenarios the time-to-capsize can be very sensitive to the initial condition. A rather marginal difference in the initial steady heel angle between the Cases 2a and 2b results in a large difference in the development of the roll angle, and especially in the eventual time-to-capsize. Although it should be noted that for the Case 2b the experiments were limited to a single test. In general, the details of the flooding and capsizing are not very well captured by the simulation methods, however, the final outcome, i.e. capsizing, is still correctly predicted. It is also noted that in the studied cases the simulations predict shorter TTC than measured, which is conservative.

## 7. Gradual flooding in waves (Case 3)

The third part of the benchmark study focused on a flooded ship motions in high waves. In the beginning of the tests the whole breach (shown in Fig. 3) is already open and the damaged compartments below the main vehicle deck (R1, R2, R4 and R5) are already flooded, and open to sea. Contrary to the transient flooding cases, also the double bottom compartments, R4 and R5 in Fig. 2, are flooded.

Two different sea states were studied, with JONSWAP wave spectrum with  $\gamma = 3.3$ . The intact condition and the significant wave heights  $H_s$  and peak periods  $T_p$  are given in Table 7. The model is in beam seas with the breach facing the waves. The model was freely drifting with loose ropes in the bow and stern for correcting the model orientation in the waves when necessary. The tests were repeated 20 times in different realizations of the same sea state. Each participant used their own codes for generating 20 random wave realizations. Maximum time for both experiments and simulations was 30 min (full scale) as in the Stockholm Agreement model tests, EU (2003).

The capsize occurs when a critical amount of water accumulates on the vehicle deck. To a significant extent the center casing reflects the waves and water flows back to the sea through the breach and the floodwater gradually spreads in the longitudinal direction on the starboard side of the vehicle deck. Video capture on the critical flooding of the deck in 3.5 m sea state is shown in Fig. 16.

Measured and simulated time histories for the roll motion in 20 realizations of both studied sea states are presented in Fig. 17 and Fig. 18. Cumulative distributions for the time-to-capsize are shown in Fig. 19. It is noteworthy that in all cases the capsize direction is towards the breach opening. The capsize rates are listed in Table 8.

The simulations by HSVA, with method based on the shallow water equations, seem to capture the capsize rate in waves due to gradual flooding qualitatively correctly in both studied sea states. In general, the HSVA results are slightly conservative with shorter time-to-capsize and larger capsize rate. In the smaller wave height (Case 3a), KRISO predicts zero capsize rate, and in the higher waves (Case 3b) either rapid capsize or survival. Interestingly, MARIN simulations are good in the smaller wave height (Case 3a), with only a small overestimation of the capsize rate, but in high waves (Case 3b) the capsize rate is significantly lower than in the model tests. MSRC predicts too low capsize rate in the

smaller wave height (Case 3a), but in the high waves (Case 3b) the time-to-capsize and capsize rate are predicted rather accurately, although the capsize rate is overestimated.

## 8. Discussion

Damage stability model tests are complex to execute, and they require a lot of expertise. Unique tests were conducted in the EU Horizon 2020 project FLARE, that enabled a detailed benchmark study. In the transient flooding (Cases 1 and 2) the damaged ropax ship rolled towards the intact side, which could not be captured by the simulation codes based on more simplified treatment of floodwater with horizontal waterplanes. It should be noted that this phenomenon is characteristic to flooding of wide undivided compartments with a large breach opening, and this is not specifically limited to ropax vessels. Previously, [Manderbacka and Ruponen \(2016\)](#) have noted that such transient effects are significant when the internal openings are of the same size as the breach opening. Due to the nature of the model test arrangement, the compartments were empty. In real ships, such wide empty compartments are not typical, and the internal non-watertight structures and equipment affect the flooding characteristics. Consequently, some of the phenomena seen in the presented model tests are expected to be less pronounced in full scale flooding.

Also, capsize due to transient flooding in irregular beam seas in the Case 2 was properly captured by most simulation codes, but the capsize mechanism was in many cases very different from the model test result. However, both the shallow water equations (SWE) and advanced pendulum models were found to provide reasonably good results. It was also found out that the time-to-capsize was rather sensitive to a small initial heel angle of the intact ship, both in model tests and simulations.

Transient flooding of wide compartments involves complex phenomena, which in this study could only be captured with advanced pendulum models or with codes based on shallow water equations. However, capsizing could also be properly predicted with some simpler methods with horizontal water levels in compartments. The challenge in modelling transient flooding of large open compartments is the evolution of the distribution of floodwater in time, as this can have a significant impact on the time-dependent heeling moment due to flooding. On the other hand, in transient flooding cases the final outcome, i.e. survival or capsize, was properly predicted by most codes, but the actual capsize mechanism and accurate time-to-capsize were much more difficult to model. Consequently, the general use of such tools for survivability assessment is reasonable, but it is also concluded that more research and validation studies are needed, especially concerning transient flooding. The sensitivity of the results to small variations in the initial condition should also be studied.

In this benchmark study more different simulation codes were used than in the previous ones. Many new codes have been introduced recently, and old ones have been improved. This benchmark study focused more on extreme conditions, including significant transient flooding and extreme sea state for gradual flooding in waves. Consequently, it is difficult to compare the results between different benchmark studies.

It was also observed that the computational performance of different simulation codes varied significantly. Detailed comparison is not possible, mainly because of different computer hardware, but also due to the different methods and their implementation, including the applied programming framework. In general, all simulations were faster than real time, and HSVA, KRISO, NAPA and UAK reported computation times over 10-times faster than simulated time. HSVA and KRISO reached this also for transient flooding in waves.

## 9. Conclusions

Time-domain simulation of flooding and motions of damaged ships is becoming a common practice for assessment of survivability level

during the ship design process, especially for passenger ships. Consequently, it is essential that such simulation codes are thoroughly validated against dedicated model tests. For this purpose, an extensive benchmark study on flooding and motions of a damaged ropax vessel was conducted within the Horizon 2020 project FLARE.

The results for the capsize rate and time-to-capsize in the case of gradual flooding in waves were characterized by a significant variability among the applied simulation codes. With some codes, the capsize rate was seriously underestimated also in a very reasonable sea state with significant wave height of 3.5 m. Consequently, survivability assessments with these tools may provide too optimistic results, and the limitations and deficiencies of the applied codes should always be considered before making any conclusions on the survivability level of a ship design.

The results show that time-domain flooding simulations are a useful tool for both research and practical ship design, although there is still a need for further development. The results of the benchmark study also clearly indicate that more research is still needed to accurately model the damaged ship dynamics in extreme environmental conditions. For example, benchmarking of intact ship motions in irregular beam seas should be conducted to conclude whether the inaccuracies in the capsizing due to gradual flooding in waves are due to hydrodynamics or treatment of floodwater. Furthermore, a repetition of the benchmark study should be considered in the future, when the existing simulation codes have been improved, or new ones have been developed.

## CRedit authorship contribution statement

**Pekka Ruponen:** Conceptualization, Methodology, Writing – original draft, Visualization, Writing – review & editing. **Petri Valanto:** Conceptualization, Investigation, Writing – review & editing. **Maria Acanfora:** Investigation, Writing – review & editing. **Hendrik Dankowski:** Investigation, Writing – review & editing. **Gyeong Joong Lee:** Investigation, Writing – review & editing. **Francesco Mauro:** Investigation, Writing – review & editing. **Alistair Murphy:** Investigation, Writing – review & editing. **Gennaro Rosano:** Investigation, Writing – review & editing. **Riaan van't Veer:** Investigation, Writing – review & editing.

## Declaration of Competing Interest

The authors declare that they have no known competing financial interests or personal relationships that could have appeared to influence the work reported in this paper.

## Acknowledgement

The research presented in this paper was carried out within the framework of the project Flooding Accident Response (FLARE), no. 814753, funded by the European Union under the Horizon 2020 program, which is gratefully acknowledged. The ropax design was kindly provided by Meyer Turku. The views set out in this paper are solely those of the authors and do not necessarily reflect the views of their respective organizations.

## References

- Acanfora, M., Cirillo, A., 2016. A simulation model for ship response in flooding scenario. *Proc. Inst. Mech. Eng. Part M J. Eng. Marit. Environ.* 231 (1), 153–164. <https://doi.org/10.1177/1475090215627839>.
- Acanfora, M., Cirillo, A., 2017. On the development of a fast modeling of floodwater effects on ship motions in waves. *Proc. Inst. Mech. Eng. Part M J. Eng. Marit. Environ.* 231 (4), 877–887. <https://doi.org/10.1177/1475090216687438>.
- Acanfora, M., De Luca, F., 2016. An experimental investigation into the influence of the damage openings on ship response. *Appl. Ocean Res.* 58, 62–70. <https://doi.org/10.1016/j.apor.2016.03.003>.

- Acanfora, M., De Luca, F., 2017. An Experimental investigation on the dynamic response of a damaged ship with a realistic arrangement of the flooded compartment. *Appl. Ocean Res.* 69, 191–204. <https://doi.org/10.1016/j.apor.2017.11.002>.
- Acanfora, M., Begovic, E., De Luca, F., 2019. A fast simulation method for damaged ship dynamics. *J. Marine Sci. Eng.* 7 (4), 1–14. <https://doi.org/10.3390/jmse7040111>.
- Acanfora, M., Rizzuto, E., 2019. Time domain predictions of inertial loads on a drifting ship in irregular beam waves. *Ocean Eng.* 174, 135–147. <https://doi.org/10.1016/j.oceaneng.2019.01.051>.
- Bačkalov, I., Bulian, G., Cichowicz, J., Eliopoulou, E., Konovessis, D., Leguen, J.-F., Rosén, A., Themelis, N., 2016. Ship stability, dynamics and safety: Status and perspectives from a review of recent STAB conferences and ISSW events. *Ocean Eng.* 116, 312–349. <https://doi.org/10.1016/j.oceaneng.2016.02.016>.
- Chang, B.-C., Blume, P., 1998. Survivability of damaged Ro-Ro passenger vessels. *Ship Technol. Res.* 45, 105–112.
- Bird, H., Browne, R.P., 1974. Damage Stability Model Experiments. *Trans. Royal Institution Naval Architects* 116, 69–91.
- Chang, B.-C., 1999. On the damage survivability of ro-ro ships investigated by motion simulation in a seaway. *Ship Technol. Res.*, 46, 192–27.
- Dand, I.W., 1991. Experiments with a floodable model of a RO-RO passenger ferry. In: *Proceedings of the Int. Conference on Ro-Ro Safety and Vulnerability the Way Ahead*. Royal Institution of Naval Architects, London, UK, 17–19 April 1991.
- Damsgaard, A., Schindler, M., 1996. In: *Proceedings of the Model Tests for Determining Water Ingress and Accumulation, International Conference on the Safety of Passenger Ro-Ro Vessels*. Royal Institute of Naval Architects, London, UK, 7th June 1996.
- Dankowski, H., 2013. A Fast And Explicit Method For The Simulation Of Flooding And Sinkage Scenarios On Ships. Hamburg University of Technology. PhD Thesis at. <http://tore.tuhh.de/handle/11420/1127>.
- Dankowski, H., Dilger, H., 2013. Investigation of the mighty servant 3 accident by a progressive flooding method. *Int. Conf. on Offshore Mechanics and Arctic Eng.*
- Dankowski, H., Russell, P., Krüger, S., 2014. New insights into the flooding sequence of the Costa Concordia accident. *Int. Conf. on Offshore Mechanics and Arctic Eng.*
- Dankowski, H., Krüger, S., 2015. Dynamic Extension of a Numerical Flooding Simulation in the Time-Domain, 12th Int. Conf. on the Stability of Ships and Ocean Vehicles STAB2015, Glasgow, UK.
- EU 2003. Directive 2003/25/EC of the European Parliament and of the Council of 14 April 2003 on specific stability requirements for ro-ro passenger ships. <https://eur-lex.europa.eu/legal-content/EN/TXT/PDF/?uri=CELEX:32003L0025&from=en>.
- Hashimoto, H., Kawamura, K., Sueyoshi, M., 2017. A numerical simulation method for transient behavior of damaged ships associated with flooding. *Ocean engineering*, 143, 282–294. [10.1016/j.oceaneng.2017.08.006](https://doi.org/10.1016/j.oceaneng.2017.08.006).
- Jasionowski, A., 2001. An integrated approach to damage ship survivability assessment. University of Strathclyde. PhD thesis. [http://oleg.lib.strath.ac.uk/?func=dbin-jump-full&object\\_id=20411](http://oleg.lib.strath.ac.uk/?func=dbin-jump-full&object_id=20411).
- Journée, J.M.J., Vermeer, H., Vredeveldt, A.W., 1997. Systematic Model Experiments of Flooding of Two Ro-Ro Vessels. In: *Proceedings of the 6th International Conference on Stability of Ships and Ocean Vehicles STAB 97*. Varna, Bulgaria. Sept. 22–27.
- de Kat, J., Kanerva, M., van't Veer, R., Mikkonen, I., 2000. Damage survivability of a new Ro-Ro ferry. In: *Proceedings of the 7th International Conference on Stability of Ships and Ocean Vehicles STAB 2000*. Launceston, Tasmania, Australia, pp. 363–384.
- Khaddaj-Mallat, C., Rousset, J.M., Ferrant, P., 2011. The transient and progressive flooding stages of damaged Ro-Ro vessels: A systematic review of entailed factors. *J. Offshore Mech. Arct. Eng.* 133 (3) <https://doi.org/10.1115/1.4002737>.
- Lee, D., Hong, S.Y., Lee, G.J., 2007. Theoretical and experimental study on dynamic behavior of a damaged ship in waves. *Ocean Eng.* 34 (1), 21–31. <https://doi.org/10.1016/j.oceaneng.2006.02.002>.
- Lee, G.J., 2015a. Flow Model for Flooding Simulation of a Damaged Ship. In: *Proceedings of the 12th International Conference on the Stability of Ships and Ocean Vehicles (STAB 2015)*, pp. 931–951. Glasgow, UK.
- Lee, G.J., 2015b. Dynamic orifice flow model and compartment models for flooding simulation of a damaged ship. *Ocean Eng.* 109, 635–653. <https://doi.org/10.1016/j.oceaneng.2015.09.051> <https://doi.org/>.
- Lorkowski, O., Dankowski, H., Kluwe, F., 2014. An experimental study on progressive and dynamic damage stability scenarios. In: *Proceedings of the ASME 2014 33rd International Conference on Ocean, Offshore and Arctic Engineering*. American Society of Mechanical Engineers Digital Collection. <https://doi.org/10.1115/OMAE2014-23388>.
- Manderbacka, T., Ruponen, P., Kulovesi, J., Matusiak, J., 2015. Model experiments of the transient response to flooding of the box shaped barge. *J. Fluids Struct.* 57, 127–143. <https://doi.org/10.1016/j.jfluidstructs.2015.06.002>.
- Manderbacka, T., Ruponen, P., 2016. The impact of the inflow momentum on the transient roll response of a damaged ship. *Ocean Eng.* 120, 346–352. <http://doi.org/10.1016/j.oceaneng.2016.02.012>.
- Manderbacka, T., Themelis, N., Bačkalov, I., Boulougouris, E., Eliopoulou, E., Hashimoto, H., Konovessis, D., Leguen, J.-F., Míguez González, M., Rodríguez, C.A., Rosén, A., Ruponen, P., Shigunov, V., Schreuder, M., Terada, D., 2019. An overview of the current research on stability of ships and ocean vehicles: the STAB2018 perspective. *Ocean Eng.* 186, 1–16. <https://doi.org/10.1016/j.oceaneng.2019.05.072>. Article 106090.
- Middleton, E.H., Numata, E., 1970. Tests of a Damaged Stability Model in Waves. SNAME Spring Meeting, Washington, DC. Paper No1970, April 1–3.
- Molyneux, D., Rousseau, J., Cumming, D., Koniecki, M., 1997. Model experiments to determine the survivability limits of damaged RO-RO ferries in waves. *Trans. Soc. Naval Architects Marine Eng.* 105, 297–321.
- Papanikolaou, A., Zaraphonitis, G., Spanos, D., Boulougouris, E., Eliopoulou, E., 2000. Investigation into the Capsizing of Damaged Ro-Ro Passenger Ships in Waves. In: *Proceedings of the 7th International Conference on Stability of Ships and Ocean Vehicles STAB 2000*. Launceston, Tasmania, Australia, pp. 351–362.
- Papanikolaou, A., Spanos, D., 2001. Benchmark study on the capsizing of a damaged Ro-Ro passenger ship in waves – final report.
- Papanikolaou, A., Spanos, D., 2005. The 24th ITTC benchmark study on numerical prediction of damage ship stability in waves – final report.
- Papanikolaou, A.D., 2007. Review of damage stability of ships – recent developments and trends. In: *Proceedings of the 10th International Symposium on Practical Design of Ships and Other Floating Structures (PRADS)*. Houston, USA; October 2007.
- Papanikolaou, A., Spanos, D., 2008. Benchmark Study on Numerical Codes for the Prediction of Damage Ship Stability in Waves. In: *Proceedings of the 10th International Ship Stability Workshop ISSW2008*. Korea.
- Pucill, K.F., Velschou, S., 1990. RO-RO passenger ferry safety studies - model test of a typical ferry. In: *Proceedings of the Int. Symposium on the Safety of Ro-Ro Passenger Ships*. Royal Institution of Naval Architects, London, 26–27 April 1990.
- Ruponen, P., 2007. Progressive Flooding of a Damaged Passenger Ship, Dissertation for the degree of Doctor of Science in Technology. Helsinki University of Technology. TTK Dissertations 94, 124 p. <https://aaltodoc.aalto.fi/handle/123456789/2931>.
- Ruponen, P., Sundell, T., Larmela, M., 2007. Validation of a simulation method for progressive flooding. *Int. Shipbuilding Progress* 54, 305–321.
- Ruponen, P., Kurvinen, P., Saisto, I., Harras, J., 2010. Experimental and numerical study on progressive flooding in full-scale. *Trans. Royal Institution Naval Architects* 152 (Part A4), A-197–207. *International Journal of Maritime Engineering*.
- Ruponen, P., 2014. Adaptive time step in simulation of progressive flooding. *Ocean Eng.* 78, 35–44. <https://doi.org/10.1016/j.oceaneng.2013.12.014> <https://doi.org/>.
- Ruponen, P., van Basten Batenburg, R., Bandringa, H., Braidotti, L., Bu, S., Dankowski, H., Lee, G.J., Mauro, F., Murphy, A., Rosano, G., Ruth, E., Tompuri, M., Valanto, P., van't Veer, R., 2021. Benchmark study on simulation of flooding progression. In: *Proceedings of the 1st International Conference on the Stability and Safety of Ships and Ocean Vehicles*. Glasgow, Scotland, UK.
- Schindler, M., 2000. Damage stability tests with models of ro-ro ferries – a cost effective method for upgrading and designing ro-ro ferries. *Contemporary Ideas on Ship Stability*. Elsevier, pp. 213–224.
- Spouge, J. R. 1986. The technical investigation of the sinking of the Ro-Ro Ferry European gateway, *Transactions of Royal Institution of Naval Architects, RINA*, Vol. 128, pp. 49–72.
- Vassalos, D., Vassalos, D., et al., 2000. The water on deck problem of damage Ro-Ro ferries. *Contemporary Ideas On Ship Stability*, pp. 163–185.
- van't Veer, R., van den Berg, J., Boonstra, S., van Basten-Batenburg, R., Bandringa, H., 2021. A steady and unsteady internal flooding model utilizing a network and graph solver. In: *Proceedings of STAB&S 2021*.
- van Walree, F., Papanikolaou, A., 2007. Benchmark study of numerical codes for the prediction of time to flood of ships: Phase I. In: *Proceedings of the 9th International Ship Stability Workshop ISSW2007*. Hamburg, Germany.
- Ypma, E.L., Turner, T., 2019. An approach to the validation of ship flooding simulation models. *Contemporary Ideas on Ship Stability*, pp. 637–675. [https://doi.org/10.1007/978-3-030-00516-0\\_38](https://doi.org/10.1007/978-3-030-00516-0_38).